RSC Advances

PAPER

View Article Online
View Journal | View Issue

Cite this: *RSC Adv.*, 2017, **7**, 11852

Catalytic reduction of NACs by nano Fe_3O_4/quinone composites in the presence of a novel marine exoelectrogenic bacterium under hypersaline conditions†

Haikun Zhang[ab] and Xiaoke Hu*[a]

Bioremediation of N-substituted aromatic compounds (NACs) has attracted a substantial amount of interest due to its cost effectiveness and environmental friendliness. However, the slow anaerobic NACs' reduction rate and the large amount of salt in wastewater are bottlenecks for biotechnology applications. In this study, a novel marine strain, *Shewanella* sp. CNZ-1, capable of reducing NACs under hypersaline conditions was isolated. To enhance the NACs reduction rate, two Fe_3O_4/quinone nanocomposites were first prepared *via* a mild covalent chemical reaction. SEM-EDX, FTIR, XRD, XPS, TG and VSM analyses were performed to illustrate the reaction process. The catalytic results showed that Fe_3O_4/2-carboxyl-anthraquinone (Fe_3O_4@COOHQ) exhibited a better catalytic performance in typical NACs bioreduction compared to Fe_3O_4/1,4-diamino-anthraquinone in the presence of strain CNZ-1. The NC reduction rates were approximately 2.2- to 6.5-fold higher than those lacking Fe_3O_4@COOHQ at 2–11% NaCl. The highest NC removal rate of 79.4 mg per h per g cell was achieved at 3% NaCl. The increased NC reduction rate is mainly due to the fact that Fe_3O_4@COOHQ could increase the NC reduction activity of cell membrane proteins containing dominant NC reductases. These findings indicate that strain CNZ-1 and Fe_3O_4@COOHQ could be used in designing a bioreactor for enhancing the treatment of NAC-containing wastewater containing a high concentration of salts.

Received 10th January 2017
Accepted 12th February 2017

DOI: 10.1039/c7ra00365j

rsc.li/rsc-advances

1. Introduction

N-Substituted aromatic compounds (NACs), including nitro-aromatics and azo dyes *etc.*, are aromatic compounds that have nitrogen atoms attached to their ring carbons, and are widely used in medicine, the chemical industry, dyes, pesticides and many other fields.[1,2] The extensive use of NACs results from their ubiquitous distribution in environment, and may have potential for eliciting a variety of adverse cytotoxic, mutagenic and carcinogenic responses.[1–3] Thus, the proper treatment of the related industrial effluents should be carried out before their release into natural water sources. In most cases, bio-treatment constitutes the primary mechanism for NAC removal due to its eco-friendliness and low cost. It was proved that anaerobic/aerobic biotreatment processes are the most widely used technologies for NAC removal.[4] In the presence of different kind of microorganisms, NACs first convert metabolically to aromatic amines under anaerobic conditions, and then mineralization of aromatic amines happens under aerobic conditions.[1,2,5] Nevertheless, there are bottlenecks for further application of these biotreatment programs: first, the anaerobic reduction of the nitrogen-containing group (*e.g.*, $-NO_2$, $-N{=}N-$) of NACs is the rate-limiting step in the NAC biodegradation process; second, the industrial effluent contains large amounts of salts,[6,7] which may decrease the activity of microorganisms.

Previous studies had demonstrated that immobilized quinone compounds (IQCs) could enhance the bioreduction of various NACs,[8] including azo dyes[8,9] and nitroaromatics,[8,10] even under saline conditions.[11,12] Moreover, compared to soluble quinone compounds (QCs), IQCs need not to be continuously added into reaction systems, which could reduce running cost and avoid secondary contamination. Therefore, the application of IQCs is a promising strategy for efficient NACs removal. So far, various carriers were developed for immobilizing QCs, mainly including polymers[9,10,13,14] and metal oxides.[11,15,16] Although many IQCs seemed to perform pretty good catalytic activity than the soluble QCs, their performance still need to further improved.[8] Recent interest in nanotechnology has provided a wealth of diverse nanoscaffolds that could potentially support QCs immobilization.[17] Fe_3O_4 is easy to prepare

[a]*Yantai Institute of Costal Zone Research, Chinese Academy of Sciences, Yantai 264000, China. E-mail: xkhucas@163.com; Fax: +86 535 2109127; Tel: +86 535 2109127*

[b]*Key Laboratory of Industrial Ecology and Environmental Engineering, Ministry of Education, School of Environmental Science and Technology, Dalian University of Technology, Dalian 116024, China*

† Electronic supplementary information (ESI) available: Materials and methods and Fig. S1–S5. See DOI: 10.1039/c7ra00365j

and recycle, and thus is an ideal carrier. In addition, ligands on surface of Fe_3O_4 could be designed and synthesized in different structures. Herein, Fe_3O_4 was selected as a carrier, and Fe_3O_4/quinone nanocomposites were prepared by using a mild covalent chemical reaction. For the other challenge, marine bacteria with good salt tolerance can be used to adapt high salt conditions. In addition, NACs are always with high polarity and hard to get into cells.[1,18] Typically, exoelectrogenic microbes possess specific extracellular electron transfer pathways, and could transfer electrons generated from substrate catabolism to terminals outside the cells.[19–21] Accordingly, marine exoelectrogenic microbes are appropriate candidates for NACs anaerobic bioreduction under saline conditions.

In this paper, Fe_3O_4/quinone nanocomposites were first synthesized *via* a covalent chemical combination method and a novel marine indigenous exoelectrogenic bacterium *Shewanella* sp. CNZ-1 was isolated for treating typical NACs, including new coccine (NC) and 2,5-dichloronitrobenzene (2,5-DCNB). The purpose of this study is to develop novel IQCs and to investigate the effect of Fe_3O_4/quinone nanocomposites as solid mediators on NACs bioreduction by strain CNZ-1 under saline conditions. During this process, the catalytic mechanism of NC reduction by strain CNZ-1 coupled with nano Fe_3O_4/quinone composite was also investigated.

2. Materials and methods

2.1 Chemicals

NC, 2,5-DCNB, anthraquinone-2-carboxylic acid (COOHQ), 1,4-diaminoanthraquinone (NH_2Q) and 1-(3-dimethylaminopropyl)-3-ethylcarbodiimide hydrochloride (EDC) used in this study were purchased from Shanghai Macklin Biochemical Co., Ltd (China). The cellulose ester dialysis membrane (100–500 D) was purchased from Shanghai Yuanye Biotechnology Co., Ltd (China). All other reagents used in this study were of the highest analytical grade.

2.2 Isolation, identification and cultivation of halotolerant exoelectrogenic bacteria

The marine sediment was taken in the middle of Bohai straits (N 38° 30.29′, E 121° 14.10′, China). Firstly, with NC served as an electron acceptor (from 0.5 to 2 g L^{-1}), the sediment was cultured and acclimated in 2216E medium for a week. Sequentially, the marine indigenous bacteria were isolated using a dilution plate method at 30 °C. The exoelectrogenic ability of the obtained bacterium was tested on the basis of the method described by Larsen.[22] Briefly, a dialysis membrane (100–500 D) was employed to separate 1 mL strain cells (OD_{600} = 1.141) from 0.1 mM NC (>500 D), the bacterium with the highest NC reduction rate without direct contact was selected for further study. In this study, the strain CNZ-1 was thus selected and identified by scanning electron microscope (SEM) and 16S rRNA gene sequencing analysis.

LB medium (LBM) contains (g L^{-1}): 10.0 peptone, 5.0 yeast extract, 10NaCl. The modified 2216E medium (M2216EM) used in this study contains (g L^{-1}): 5.0 peptone, 1.0 yeast extract, 0.1 ferric citrate, 20–90NaCl, 5.98$MgCl_2$, 3.24Na_2SO_4, 1.8$CaCl_2$, 0.55KCl, 0.16Na_2CO_3, 0.08KBr, 0.034$SrCl_2$, 0.022H_3BO_3, 0.004Na_2SiO_3, 0.0024NaF, 0.0016$NaNO_3$, 0.008Na_2HPO_4, aged-seawater. The mineral salt medium (MSM) used in this study contains (g L^{-1}): 1.0$(NH_4)_2SO_4$, 0.8Na_2HPO_4, 0.2KH_2PO_4, 0.2$MgSO_4 \cdot 7H_2O$, 0.1$CaCl_2 \cdot 2H_2O$, 20–110NaCl.

2.3 Preparation of Fe_3O_4/quinone nanocomposites and their characterisation

Fe_3O_4 nanoparticle was synthesized according to the method described in the ESI.† Fe_3O_4@NH_2Q nanocomposite was prepared by the following steps: (i) 1.0 g Fe_3O_4 nanoparticles and 20 mL buffer solution (BS, including 3 mM phosphoric acid and 100 mM NaCl) were mixed in a 250 mL flask. Then, 5 mL EDC solution (2.5 wt%, with the treatment of light avoidance) was added. After 20 min sonication, 25 mL polyacrylamide solution (6 wt%) were added and reacted for 2 h at 25 °C. The product (Fe_3O_4–COOH) was separated by magnet and washed with deionized water. (ii) 0.2 g NH_2Q was dissolved in 200 mL deionised water (95% ethanol was added to help dissolve the NH_2Q, pH = ~8) by water bath sonication for 1 h. Then, 1.0 g Fe_3O_4–COOH, 45 mL BS and 5 mL EDC solution were first mixed by water bath sonication for 20 min at 25 °C. Sequentially, the mixture were added to the NH_2Q solution in a 500 mL round-bottom flask. The flask was placed in a water bath at 98 °C and stirred for ~24 h. The products was cooled to room temperature and washed with deionised water and 50% ethyl alcohol *via* filtration using cellulose ester dialysis membranes to remove the excess NH_2Q.

Fe_3O_4@COOHQ nanocomposite was prepared by the following steps: (i) 1.0 g Fe_3O_4–COOH, 45 mL BS and 5 mL EDC solution were mixed in a 250 mL flask. After 20 min sonication, 5 mL diethylenetriamine was added and reacted for 2 h in a water bath of 98 °C. The products (Fe_3O_4–NH_2) were separated by magnet, washed with deionized water and dissolved in 200 mL deionised water with sonication treatment for 1 h. (ii) Then, 0.2 g COOHQ, 45 mL BS and 5 mL EDC solution were first mixed by water bath sonication for 20 min at 25 °C. Sequentially the mixture were added to the Fe_3O_4–NH_2 solution (pH = ~8) in a 500 mL round-bottom flask. The flask was placed in a water bath at 98 °C and stirred for ~24 h. The products were cooled to room temperature and washed with deionised water and 50% ethyl alcohol *via* filtration using cellulose ester dialysis membranes to remove the excess COOHQ.

Finally, Fe_3O_4@NH_2Q and Fe_3O_4@COOHQ were dried in a vacuum freeze drying equipment for the following experiments. Scanning electron microscope-energy disperse X-ray spectroscopy (SEM-EDX, Hitachi S-4800, Japan), Fourier transform infrared spectroscopy (FTIR, Jasco FT/IR-4100, Japan), X-ray diffraction patterns (XRD, RIGAKU 18 KW, Japan) and X-ray photoelectron spectroscopy (XPS, ESCALAB 250Xi, England) were used to investigate the morphology and chemical compositional changes on the surfaces of the Fe_3O_4/quinone composites. In addition, the thermogravimetric analysis was performed using a thermal analyzer (TG, Mettler 5MP/PF7548/MET/400W, Switzerland) with a heating rate of 10 °C min. The magnetization curves of the Fe_3O_4, Fe_3O_4@NH_2Q and

Fe_3O_4@COOHQ were examined using a vibrating sample magnetometer (VSM, Lake Shore 7410, USA).

2.4 Enhanced NACs bioreduction in the presence of Fe_3O_4/quinone nanocomposites

Effects of pH (3–10) and NaCl concentration (2–9%, wt%) on growth of CNZ-1 were investigated using M2216EM under anaerobic conditions. For bioreduction assays, strain CNZ-1 was first cultured overnight in 100 mL LBM (1%, v/v) in a rotary incubator shaker at 180 rpm, 30 °C. Then, the CNZ-1 cells were harvested by centrifugation (5 min, 10 000 rpm) and washed twice with a sterile phosphate buffer solution (PBS, 10 mM, pH 7.0). At last, the cell pellets were resuspended with MSM and held in an anaerobic chamber. The experimental systems utilised 135 mL serum bottles containing 100 mL deoxygenated sterile MSM, NACs and an electron donor. The CNZ-1 cells were added into the systems at a final concentration of 0.11 g L^{-1}. After cell inoculation, samples were periodically taken with a sterile needle and a syringe for the analysis of NACs. Besides, the effects of different electron donors (glucose, formic acid, lactic acid, sucrose and acetate) on the NC reduction rates were investigated at an initial NC concentration of 0.1 mM. The effect of the optimal electron donor concentration (0–5 g L^{-1}) was also studied.

Under the above optimal conditions, the bioreduction of NC, nitrobenzene (NB), *p*-chloronitrobenzene (PCNB) and 2,5-DCNB (0.1 mM) by strain CNZ-1 (0.11 g L^{-1}) were performed in the presence of Fe_3O_4/quinone nanocomposites (60 mg L^{-1}). Control system without cells was also analysed. Moreover, the effects of different Fe_3O_4@COOHQ concentrations (5–80 mg L^{-1}) and NaCl concentrations (2–11%, in the presence of 60 mg L^{-1} Fe_3O_4@COOHQ) on the NC bioreduction rate were further investigated. Repeated batch operations were carried out to investigate the stability and persistence of Fe_3O_4@COOHQ. All treatments and controls were run in triplicate.

2.5 Preparation of cell extracts and enzyme activity assays

After strain CNZ-1 was cultivated overnight in 100 mL LBM, the cells were harvested by centrifugation (15 min, 10 000 rpm) and washed twice with a phosphate buffer (10 mM, pH 7.0). Then, cell pellets were added to 300 mL MSM (2 g L^{-1} lactate sodium and 1 mM NC) and cultured at 30 °C. After 24 h, the cells were harvested by centrifugation (15 min, 10 000 rpm). All subsequent steps were carried out at 4 °C unless otherwise stated. The obtained cells were suspended in a cold modified PBS (PBS + 10% glycerol, 2 mM EDTA and 1 mM dithiothreitol) and treated with 30 min sonication in an ice bath. Unbroken cells were removed by centrifugation (5 min, 10 000 rpm). The crude extracts were then subject to ultracentrifugation at 150 000 rpm for 2 h. The obtained precipitation was re-suspended in the phosphate buffer and used as a mixture of membrane proteins. The supernatant was used as a mixture of cytoplasmic and periplasmic proteins. The total protein content was estimated by Lowry's method.[23]

The NC reductase activity was assayed using NADH as an electron donor. The total volume of the reaction mixture was 3 mL, which contained 1 mL crude enzyme solution, 60 mg L^{-1} Fe_3O_4 or Fe_3O_4@COOHQ, 0.1 mM NADH and 0.1 mM NC in a PBS. The assay mixtures were incubated at 30 °C in an anaerobic incubator.

2.6 Analytical methods

The concentrations of cells and NC were determined by UV-Vis spectrophotometer at their characteristic absorption peaks (600 nm and 506 nm, respectively). The concentrations of NB (254 nm), PCNB (275 nm) and 2,5-DCNB (230 nm) were determined by HPLC. The reduction products were determined using HPLC-MS fitted with Sapphire C18 column (4.6 mm × 200 mm). The mobile phase consisted of methanol and water (70 : 30, v/v) at 1.0 mL min^{-1}. The reduction efficiency and rate of NACs were calculated using eqn (1) and (2), respectively, as follows:

$$\text{Reduction efficiency (\%)} = \frac{C_\text{i} - C_t}{C_\text{i}} \times 100\% \quad (1)$$

$$\text{Reduction rate} = \frac{C_\text{i} - C_\text{t}}{mt} \quad (2)$$

where C_i (mg L^{-1}) and C_t (mg L^{-1}) are the initial and residual NC at time zero and t, respectively; m (g cell per L) is the dry weight of the cells; t (h) is the reaction time.

A zero-order model was applied to describe the kinetics of NC bio-reduction. The zero-order rate constant k_1 (mol L^{-1} h^{-1}) was determined.

$$C_0 - C_t = -k_1 t \quad (3)$$

A pseudo-first-order model was used to describe the kinetics of NC bio-reduction. The first-order rate constant k_2 (h^{-1}) was determined.

$$\ln C_0/C_t = k_2 t \quad (4)$$

3. Results

3.1 Characterization of Fe_3O_4/quinone nanocomposites

The preparation schematic illustration of Fe_3O_4@NH_2Q and Fe_3O_4@COOHQ nanocomposites was shown in Fig. 1. As can be seen, the reaction conditions are mild. SEM results showed that the surface of Fe_3O_4 was smooth while the surfaces of Fe_3O_4@NH_2Q and Fe_3O_4@COOHQ were slightly rough (Fig. 2). In addition, the elemental compositions of different composites that obtained by EDX were list in Table 1. On the basis of the EDX results, the immobilization efficiencies of the two QCs are approximately 262 μmol NH_2Q per g Fe_3O_4 and 499 μmol COOHQ per g Fe_3O_4, respectively. It was noticeable that C and N elements were appeared after the related modification. To characterise the change of Fe_3O_4 nanoparticles' crystal structure before and after modification, XRD analysis was performed. For Fe_3O_4 nanoparticle, the observed XRD peaks at 2θ = 30.51°, 35.79°, 43.45°, 53.81°, 57.33° and 62.92° can be indexed to (220), (311), (400), (422), (511) and (440) planes of magnetite, respectively (Fig. 3 and JCPDS card, file no. 19-0629). The observed XRD patterns of five nanocomposites were similar, indicating

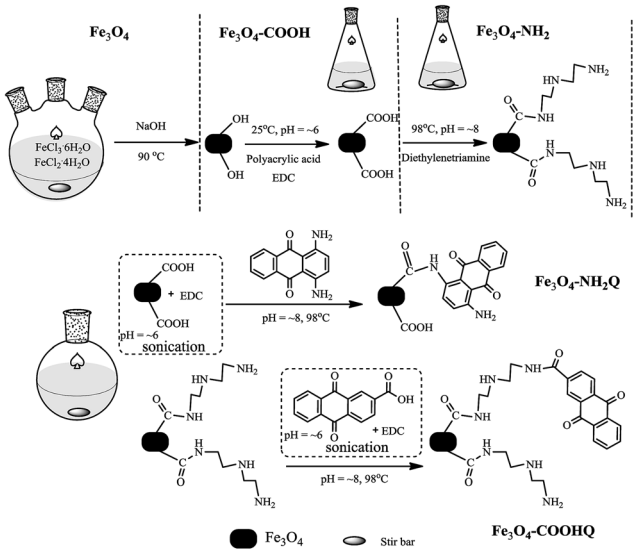

Fig. 1 The schematic illustration of the preparation of Fe_3O_4@NH_2Q and Fe_3O_4@COOHQ.

that the crystal structure of Fe_3O_4 nanoparticles were well remained after modification.

During preparation of Fe_3O_4@NH_2Q and Fe_3O_4@COOHQ, the carboxyl groups can react with the amino group, which was demonstrated by FTIR and XPS analyses. As can be seen in Fig. 4a, 559 cm^{-1} was related to the Fe–O bending vibration. The characteristic absorption bands of –COOH at approximately 1762 cm^{-1} and –CONH at approximately 1458 cm^{-1}, 1612 cm^{-1} shifted or appeared in FTIR of Fe_3O_4–COOH, Fe_3O_4–NH_2, Fe_3O_4@NH_2Q and Fe_3O_4@COOHQ, respectively. Simultaneously, the characteristic absorption bands of benzene ring at approximately 1500–1600 cm^{-1} appeared in FTIR of Fe_3O_4@NH_2Q and Fe_3O_4@COOHQ (Fig. 4a). As shown in the O 1s spectra of Fe_3O_4–COOH, Fe_3O_4–NH_2, Fe_3O_4@NH_2Q and Fe_3O_4@COOHQ, the intensity of the C=O, C–O and –OH peaks changed after different reactions compared with those in the O 1s spectrum of Fe_3O_4 (Fig. 4b–f). Moreover, it was noticeable that the intensity of the lattice oxygen peak decreased at different levels in the O 1s spectra of Fe_3O_4@NH_2Q and Fe_3O_4@COOHQ compared with those in the O 1s spectrum of the Fe_3O_4, indicating that the surface of Fe_3O_4 was probably partially covered with NH_2Q and COOHQ (Fig. 4b, e and f). Besides, the appearance of an N 1s peak at 390–400 eV was also observed in the spectra of the Fe_3O_4–NH_2, Fe_3O_4@NH_2Q and Fe_3O_4@COOHQ (data not shown). All these observations also suggest the successful surface modification of the Fe_3O_4 by the NH_2Q and COOHQ molecules.

Table 1 Element composition on the surface of Fe_3O_4-based nanocomposites[a]

Sample		O	Fe	C	N
Fe_3O_4	Mass (%)	31.58	61.71	—	—
	Molar (%)	68.42	38.29	—	—
Fe_3O_4–COOH	Mass (%)	30.51	67.08	2.41	—
	Molar (%)	57.64	36.31	6.05	—
Fe_3O_4–NH_2	Mass (%)	35.48	60.36	2.81	1.36
	Molar (%)	61.11	29.78	6.44	2.67
Fe_3O_4@NH_2Q	Mass (%)	23.11	73.60	2.60	0.69
	Molar (%)	47.70	43.52	7.14	1.63
Fe_3O_4@COOHQ	Mass (%)	23.97	65.24	10.79	—
	Molar (%)	42.04	32.77	25.19	—

[a] "—" not detected.

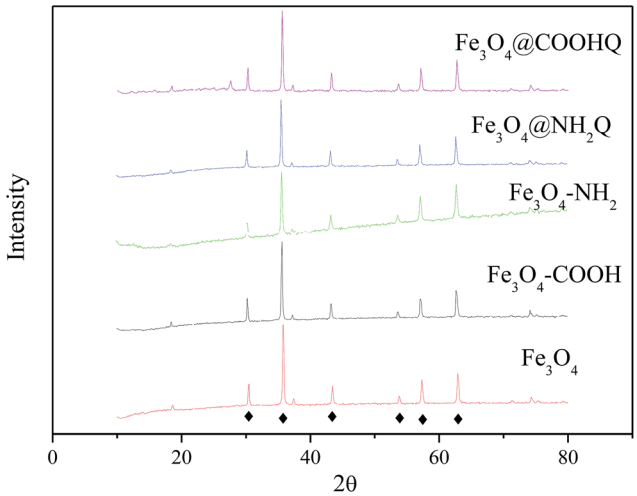

Fig. 3 XRD patterns of Fe_3O_4, Fe_3O_4–COOH, Fe_3O_4–NH_2, Fe_3O_4@NH_2Q and Fe_3O_4@COOHQ.

The TG analyses of Fe_3O_4-based composites were performed in air atmosphere and the results were shown in Fig. 5. When the temperature was over 200 °C, the weights of Fe_3O_4, Fe_3O_4–COOH and Fe_3O_4–NH_2 kept invariant. The weight loss of Fe_3O_4@NH_2Q was first appeared from 200 to 400 °C, and then appeared from 700 to 900 °C. The weight loss of Fe_3O_4@COOHQ was contained three steps: from 200 to 300 °C, from 300 to 500 °C, from 700 to 900 °C. This phenomenon may due to the thermal decomposition of the NH_2Q and COOHQ. The magnetic properties of the obtained composites were evaluated

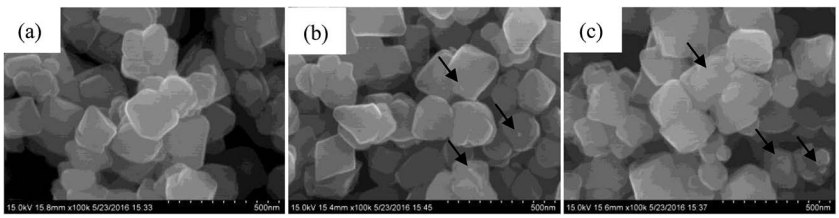

Fig. 2 The SEM images of Fe_3O_4 (a), Fe_3O_4@NH_2Q (b) and Fe_3O_4@COOHQ (c).

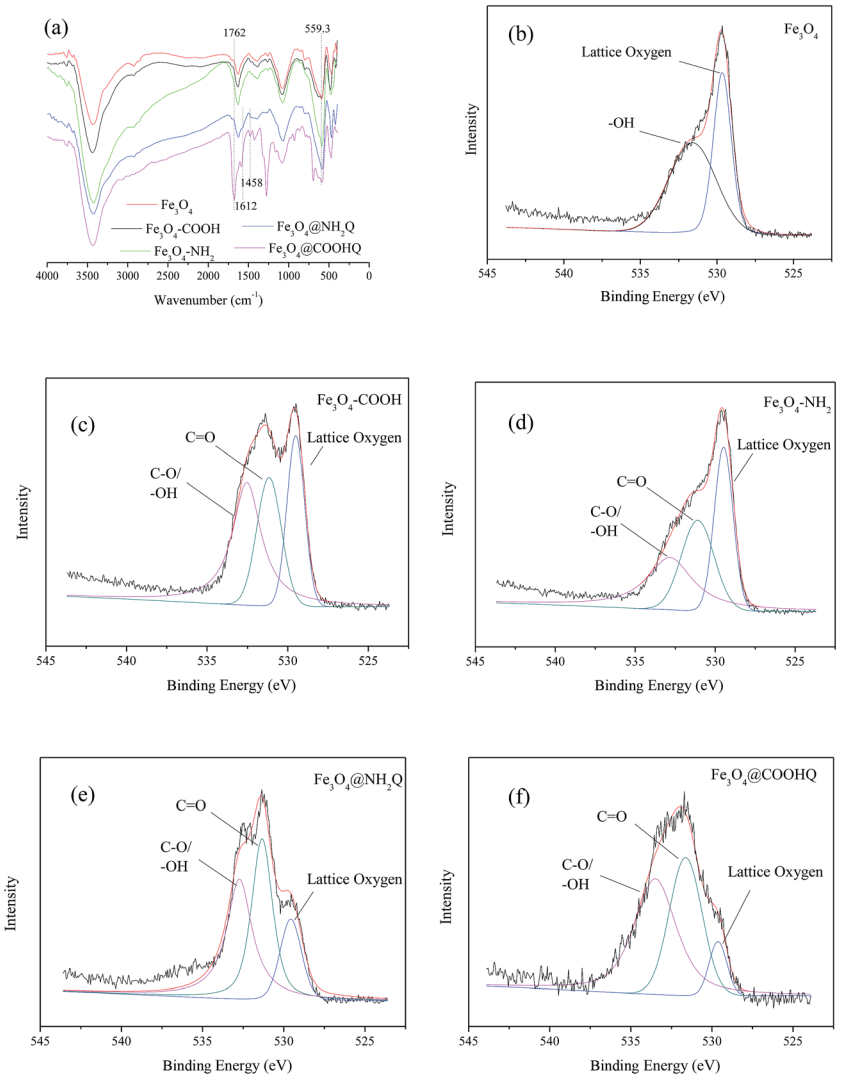

Fig. 4 FTIR spectra and XPS spectra of Fe_3O_4, Fe_3O_4–COOH, Fe_3O_4–NH_2, Fe_3O_4@NH_2Q and Fe_3O_4@COOHQ. (a) FTIR spectra of Fe_3O_4, Fe_3O_4–COOH, Fe_3O_4–NH_2, Fe_3O_4@NH_2Q and Fe_3O_4@COOHQ; (b) O 1s of Fe_3O_4; (c) O 1s of Fe_3O_4–COOH; (d) Fe_3O_4–NH_2; (e) O 1s of Fe_3O_4@NH_2Q; and (f) O 1s of Fe_3O_4@COOHQ.

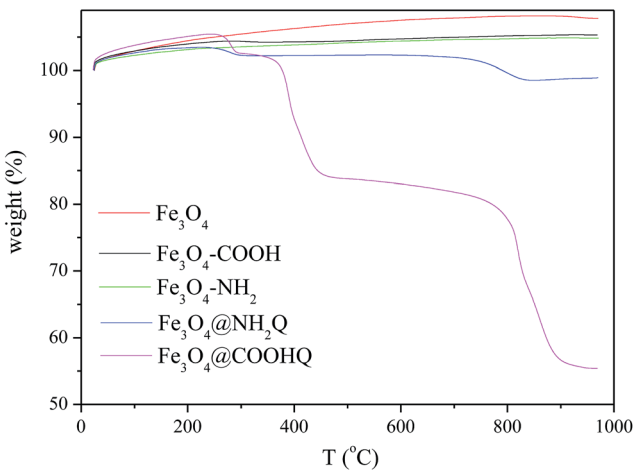

Fig. 5 TG analyses of Fe_3O_4, Fe_3O_4–COOH, Fe_3O_4–NH_2, Fe_3O_4@NH_2Q and Fe_3O_4@COOHQ.

using VSM (Fig. 6). The magnetic coercivity/or remanence values of Fe_3O_4, Fe_3O_4@NH_2Q and Fe_3O_4@COOHQ are nearly zero, indicating their superparamagnetic behaviour. The saturation magnetization of Fe_3O_4 decreased with the graft of non-magnetic NH_2Q and COOHQ. However, even so, both Fe_3O_4@NH_2Q and Fe_3O_4@COOHQ could be separated from aqueous solution effectively (Fig. 6 inset).

3.2 A newly isolated halotolerant exoelectrogenic strain

A facultative anaerobic strain capable of transferring electron to extracellular environment was isolated and named CNZ-1. As mentioned above, NC with high polarity was select as an extracellular electron acceptor to verify the exoelectrogenic ability of CNZ-1. The results showed that strain CNZ-1 trapped in the dialysis bag (1 mL) could first decolour 0.1 mM NC completely within 48 h in all 4 candidates. When strain CNZ-1 was grown on an LB agar plate under aerobic conditions, its colony was tangerine and

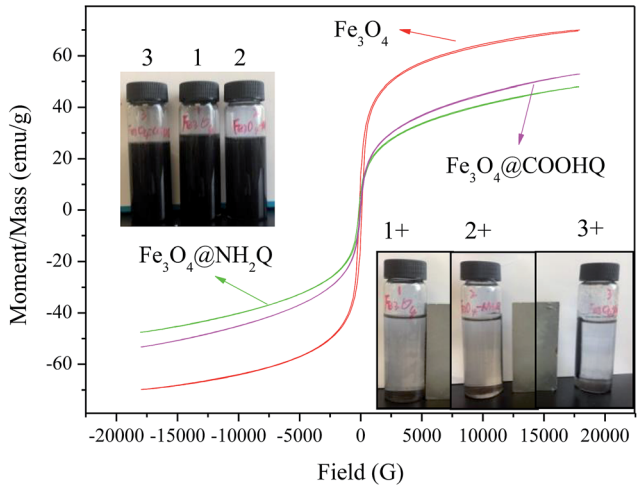

Fig. 6 VSM analyses of Fe_3O_4@NH_2Q and Fe_3O_4@COOHQ.

circular in shape (Fig. S1a†). The SEM results showed that the morphology of strain CNZ-1 is a short rod with dimensions of 2 × 0.3 μm^2 (Fig. S1b†). On the basis of the sequencing of the 16S rDNA gene, the homology between strain CNZ-1 (GenBank accession number KX384589) and a *Shewanella algae* JCM 21037 (GenBank accession number NZ_BALO01000089.1) is 99%. Thus, it can be concluded that strain CNZ-1 belongs to the genus *Shewanella*. The phylogenetic tree of strain CNZ-1 is shown in Fig. S1c.† NaCl resistance assays (2–9%) showed that the anaerobic growth in the M2216EM had only slight delay with the increase of NaCl concentration from 2 to 5% (Fig. S2a†). When adding 7% NaCl, the strain CNZ-1 could recover the growth after 18 h incubation. When adding 9% NaCl, the growth of strain CNZ-1 inhibited severely. Effect of pH on growth of CNZ-1 was investigated and the results showed that strain CNZ-1 grew best under pH 7.3, whereas it failed to survive at pH 3.8 (Fig. S2b†).

3.3 Fe_3O_4/quinone composites mediated NACs bioreduction by CNZ-1

The effect of electron donor on NC reduction was shown in Fig. S3.† Among the six electron donors, sodium lactate was proven to be the most suitable electron donor for strain CNZ-1 to reduce NC (Fig. S3a†). In addition, the NC reduction rate did not sharply increase as the concentration of sodium lactate was over 2.0 g L^{-1} (Fig. S3b†). Thus, 2.0 g L^{-1} sodium lactate was selected for the following experiments. The effects of Fe_3O_4@NH_2Q and Fe_3O_4@COOHQ on NACs reduction were further investigated. It was noticing that NC reduction rate could achieve 76.03 μmol per h per g cell in the presence of 20 mg L^{-1} Fe_3O_4@COOHQ. The highest NC reduction rate of 79.35 μmol per h per g cell could be achieved in the presence of 60 mg L^{-1}

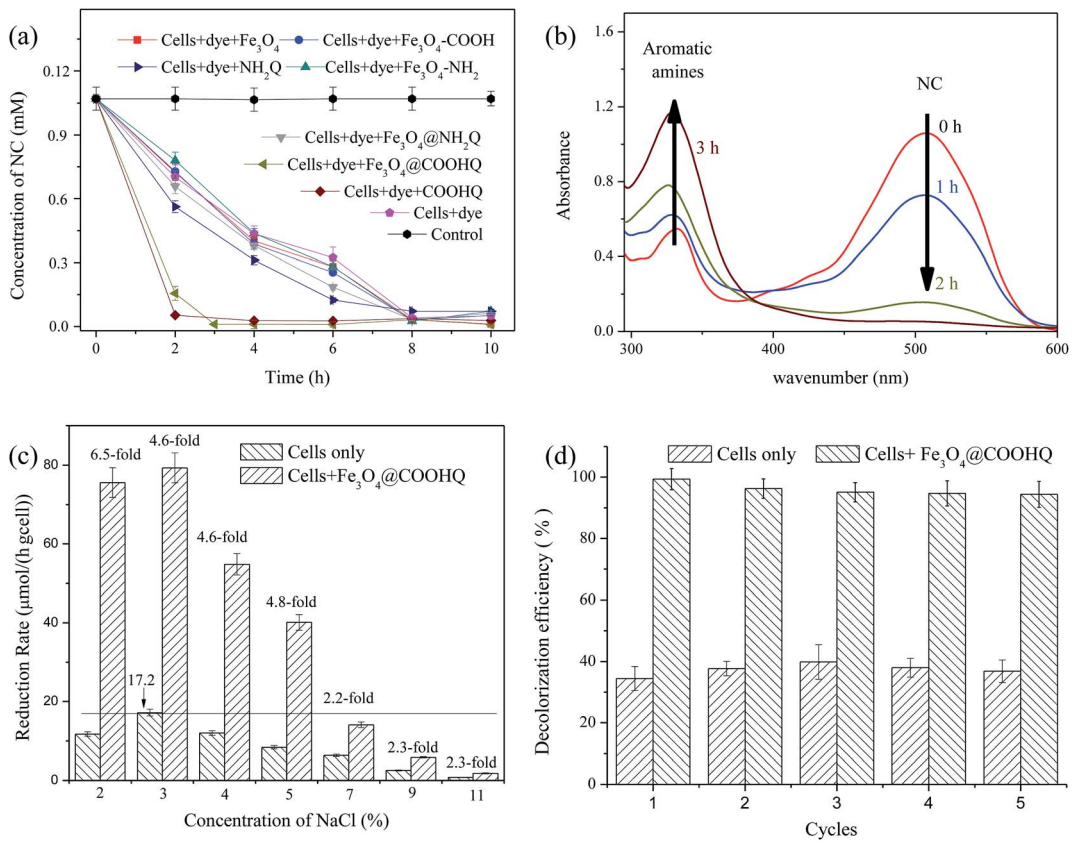

Fig. 7 Effects of Fe_3O_4@NH_2Q and Fe_3O_4@COOHQ on the NC reduction by strain CNZ-1. (a) NC reduction curves; (b) the wavelength scanning analysis of Fe_3O_4@COOHQ supplemental system; (c) effect of NaCl concentration on Fe_3O_4@COOHQ mediated NC reduction by strain CNZ-1; and (d) repeat experiment of Fe_3O_4@COOHQ. Error bars shows mean standard deviation of three determinations.

Table 2 Immobilized efficiency and catalyzing performance of different nano particle/QCs composites[a]

Nano particle carriers	QCs	Method	Concentration of QCs immobilized	Pollutants/catalytic performance	Recycle	Reference
α-Al_2O_3	AQDS	Physical	7 μmol g^{-1}	N. D.	N. D.	15
ZnO		Absorption	6 μmol g^{-1}	N. D.	N. D.	15
$Al(OH)_3$			105 μmol g^{-1}	AD/7.5-fold[b]	N. D.	15
TiO_2	FA	Physical	4.1 mg g^{-1}	N. D.	N. D.	16
$Al(OH)_3$		Absorption	2.6 mg g^{-1}	N. D.	N. D.	16
γ-Al_2O_3			12 mg g^{-1}	CT/10.4-fold[b]	N. D.	16
GO	AQS	Chemical	160 μmol g^{-1}	AD/+44%[c]	5	30
GO	NQ	Chemical	1.93 mmol g^{-1}	Cr(VI)/+90%[c]	N. D.	31
	AQ		2.69 mmol g^{-1}	Cr(VI)/+12%[c]	N. D.	31
Fe_3O_4	COOHQ	Chemical	499 μmol g^{-1}	AD/1.71-fold[d] CNB/+48%[c]	5	This study
	NH_2Q		262 μmol g^{-1}	AD/+6%[c]	N. D.	This study

[a] GO: graphene oxide; AQDS: anthraquinone-2,6-disulfonic acid sodium; FA: fulvic acids; AQS: anthraquinone-2-sulfonic acid sodium; COOHQ: anthraquinone-2-carboxylic acid; NH_2Q: 1,4-diaminoanthraquinone; NQ: 2-amino-3-chloro-1,4-naphthoquinone; AQ: 2-aminoanthraquinone; AD: azo dye; CT: carbon tetrachloride; CNB: chloronitrobenzene; N. D.: no detection is made. [b] Reduction rate. [c] Reduction efficiency. [d] Enzymic activity (membrane protein).

Table 3 The kinetic parameters for NC bioreduction mediated by Fe_3O_4@COOHQ

System	k_1 (mol L^{-1} h^{-1})	R^2	k_2 (h^{-1})	R^2	t (h)
Cell + dye	0.1135	0.9031	0.3527	0.9778	8
Cell + dye + COOHQ	0.5088	0.9516	1.5046	0.9923	2
Cell + dye + Fe_3O_4@COOHQ	0.3682	0.8681	1.4671	0.9827	3
Cell + dye + NH_2Q	0.1247	0.9161	0.4122	0.9211	6
Cell + dye + Fe_3O_4@NH_2Q	0.1236	0.8539	0.3959	0.9845	8
Cell + dye + Fe_3O_4–NH_2	0.1225	0.9087	0.4088	0.9284	8
Cell + dye + Fe_3O_4–COOH	0.1279	0.9175	0.4263	0.9676	8
Cell + dye + Fe_3O_4	0.1211	0.8972	0.3667	0.9105	8

Fe_3O_4@COOHQ, and this concentration was thus selected for the following experiments (Fig. S3c†). NC reduction (<1%) was not observed in the presence of only Fe_3O_4@NH_2Q and Fe_3O_4@COOHQ (data not shown). Strain CNZ-1 cells could only reduce ~30% NC in 2 h and the addition of 60 mg L^{-1} Fe_3O_4@COOHQ resulted in an increase in NC reduction efficiency from ~30% to over 85% in 2 h (Fig. 7a). In comparison, the Fe_3O_4@NH_2Q-mediated NC reduction rate was slower. In the presence of 60 mg L^{-1} Fe_3O_4@NH_2Q, the NC reduction efficiency was slightly increased from ~30% to ~36%. Moreover, the catalytic efficiency of dissolved QCs is higher than IQCs, owing to their homogeneous distribution. The zero-order and pseudo-first-order model were used to describe the kinetics of NC bio-decolorization mediated by Fe_3O_4@COOHQ. The kinetic parameters of the zero-order and pseudo-first-order equations were listed in Table 3. The experimental kinetic data of Fe_3O_4@COOHQ mediated NC bio-reduction fit well with the pseudo-first-order model ($R^2 > 0.98$). Fe_3O_4@COOHQ-mediated NC reduction ($k = 1.4671$ h^{-1}, $R^2 > 0.98$) was 3.7-fold higher than that mediated by Fe_3O_4@NH_2Q ($k = 0.3959$ h^{-1}, $R^2 > 0.98$), indicating that Fe_3O_4@COOHQ is a better solid mediator than Fe_3O_4@NH_2Q for NC reduction with strain CNZ-1. In addition, the full wave scanning of samples taken at 0, 1, 2 and 3 h in the Fe_3O_4@COOHQ supplemented system was shown in Fig. 7b. As can be seen, NC was gradually reduced to corresponding reduction products as time went on. The reduction products were analyzed using HPLC-MS and the reduction product was proven to be N^1-phenylbenzene-1,4-diamine (Fig. S4a†). To demonstrate the general applicability of Fe_3O_4@COOHQ for the NACs bioreduction under saline conditions, the effects of Fe_3O_4@COOHQ (60 mg L^{-1}) on NB, PCNB and 2,5-DCNB reduction (0.1 mM) by strain CNZ-1 (0.11 g L^{-1}) was also investigated in the presence of 3% NaCl. As shown in Fig. S4b,† the removal efficiency of NB, PCNB and 2,5-DCNB were about 1.6-, 1.9- and 1.7-fold higher than those lacking Fe_3O_4@COOHQ, respectively.

The effect of NaCl on Fe_3O_4@COOHQ mediated NC bioreduction was further investigated and the NC reduction process curves in the absence/presence of Fe_3O_4@COOHQ were shown in Fig. S5.† In general, the addition of Fe_3O_4@COOHQ leads to a great improvement in NC bioreduction rate under saline conditions. In the absence of Fe_3O_4@COOHQ, the highest NC reduction rate of 17.2 μmol per h per g cell could be achieved under 3% NaCl conditions (Fig. 7c). When adding 60 mg L^{-1} Fe_3O_4@COOHQ, the NC reduction rate were approximately 6.5-, 4.6-, 4.6-, and 4.8-fold higher than those lacking Fe_3O_4@COOHQ at 2, 3, 4, and 5% NaCl, respectively

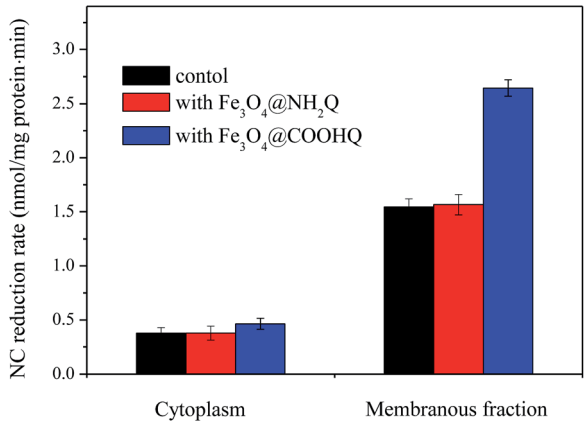

Fig. 8 NC reductase activities in cell fractions of strain CNZ-1 in three different reaction systems.

(Fig. 7c). When the NaCl concentration was over 7%, NC reduction rates were no more than 17.2 μmol per h per g cell even in the presence of Fe_3O_4@COOHQ (Fig. 7c). As shown in Fig. 7c, NC reduction rate was gradually decreased with the increasing salt concentration from 3 to 11%. It seems that NC reduction process was growth-linked, high salt concentration suppressed the growth of strain CNZ-1 and thus inhibited the rate of NC reduction.

To further study the persistence and stability of Fe_3O_4@COOHQ, repeated batch experiments were carried out in the presence of 3% NaCl. Fig. 7d showed that the reduction efficiency of Fe_3O_4@COOHQ mediated NC (0.1 mM) could remain over 94% of its original value after 5 cycles. In comparison, the reduction rate of NC in non mediator supplemented system was lower than that in Fe_3O_4@COOHQ-supplemented system during five rounds. This indicates that Fe_3O_4@COOHQ as an electron conductor holds good persistence and stability in repetitive operations.

3.4 Enzyme activity assays

NC reduction was studied with different protein factions of strain CNZ-1 (Fig. 8). No disappearance of NC was observed in control systems that lacking protein or NADH (data not shown). In addition, systems containing cytoplasmic proteins and membrane components removed ~11% and ~47% NC in 10 min with an average reduction rate of 0.37 and 1.54 nmol NC per mg protein per min, respectively. In the presence of Fe_3O_4, no obvious differences were found. In the presence of Fe_3O_4@COOHQ, systems containing cytoplasmic proteins and membrane components removed ~12% and ~80% NC in 10 min with an average reduction rate of 0.46 and 2.65 nmol NC per mg protein per min, respectively (Fig. 8).

4. Discussion

So far, a number of microorganisms have potential application for bioreduction of typical NACs under low-salt conditions, including *Bacillus* sp., *Citrobacter* sp., *Kocuria rosea*, *Shewanella oneidensis*, *Penicillium* sp. and *Sphingomona xenophaga*.[24–26] However, for example, large amounts of salts were added as accessory ingredients to improve dyeing performance in the production process of dye.[27] The dyeing baths of direct dye was reported to normally bear ~2% of mineral salts while those of reactive dye contain over 3% NaCl.[28] A previous study reported that reduction of NACs was severely inhibited when the salt concentration was higher than 3–5%.[27] Therefore, there is a dire need to isolate such NACs reducing bacterial community which could tolerate high-salt concentrations. Up to now, only a few halotolerant or halophilic bacteria were identified.[27] Since marine indigenous bacteria can survive at high salt concentration, they are the best candidates for treating NACs-containing wastewaters.[7] In the present study, a novol strain *Shewanella* sp. CNZ-1 was isolated from marine sediment and it was proven to be capable of reducing typical NAC rapidly in the presence of 2–9% NaCl. Moreover, strain CNZ-1 can tolerate less than 11% NaCl. Besides, strain CNZ-1 was also confirmed as a member of high efficient electrogenic microorganisms. The extracellular electron transfer is an essential step for reduction of some macromolecular NACs by microorganisms. Thus, strain CNZ-1 presents a potential application for the bioremediation of NACs under saline conditions.

Compared to many chemical and physical treatment technologies, bioremediation of NACs is considered as a cost-effective and environmental friendly technology. However, the biodegradation efficiencies of NACs are very low under high-salt conditions.[27] Thus, it is necessary to develop highly efficient biotreatment technologies for NACs removal. The standard potentials of QCs are considerably lower than that of most NACs, and thus the electron transfer from the reduced QCs to NACs is thermodynamically feasible. Previous studies found that IQCs could lead to a great increase in the NACs reduction rate in the presence of a mixed salt-tolerant bacterial culture.[9,12] IQCs mediated reduction of NACs mainly included two steps: (I) QCs is first reduced to hydroquinones by cells; (II) then hydroquinones reduce NACs by a purely chemical redox reaction outside the cell.[14,29] Accordingly, two kinds of nano IQCs were prepared by using a mild chemical method. Table 2 summarized the immobilized efficiency and catalyzing performance of different nano particle/QCs composites previously reported. The immobilized efficiency of Fe_3O_4@COOHQ was moderate.

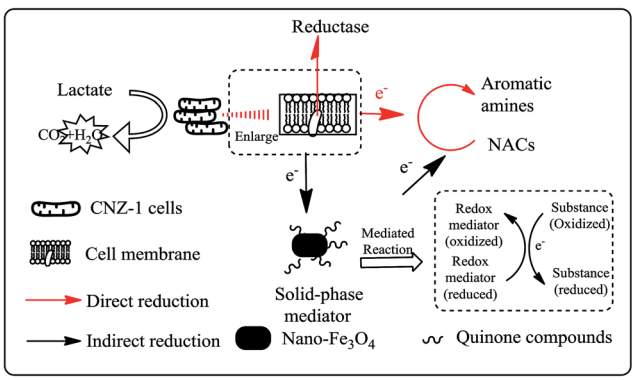

Fig. 9 The proposed mechanism of Fe_3O_4@COOHQ mediated NACs reduction by strain CNZ-1.

However, compared to other nano scale IQCs, Fe_3O_4@COOHQ could be recycled more easily due to its magnetic property. It was noticed that 60 mg L^{-1} Fe_3O_4@COOHQ could significantly increase the NC reduction rate from 17.2 to 79.4 mg per h per g cell in the presence of 0.1 mM NC and 3% NaCl. That's to say, Fe_3O_4@COOHQ exhibited a good catalytic performance in NACs bioreduction.

Previous study showed that different bacteria have different abilities to reduce QCs.[29] In the present study, catalytic performance for NC bioreduction of COOHQ was better than NH_2Q, perhaps indicating that strain CNZ-1 prefers to reduce COOHQ. In addition, further study showed that the immobilization concentration of COOHQ was higher than NH_2Q by using the mentioned method. Thus, Fe_3O_4@COOHQ was selected for further study. Fe_3O_4@COOHQ could increase the NC reduction activity of both cell membrane and extracts proteins, especially for cell membrane proteins. *Shewanella* was ever proven that there are large numbers of c-type cytochromes and reductases on and between its inner and outer membranes.[32,33] Previous study found that *Shewanella decolorationis* S12's reduction activity towards azo dye was only present in its membranous fraction.[34] Our results further indicated that the membrane-bound proteins of CNZ-1 were crucial for the reduction of NC.

Accordingly, the mechanism of Fe_3O_4@COOHQ mediated reduction of NACs was proposed: (I) NACs were reduced to the corresponding aromatic amine directly; (II) Fe_3O_4@COOHQ was first reduced by outer membrane proteins of strain CNZ-1; second, the formed hydroquinones reduced NACs to the corresponding aromatic amine in a purely chemical redox reaction; and last, hydroquinones were changed to into quinones again (Fig. 9). During this process, Fe_3O_4@COOHQ acted as a solid phase redox mediator for accelerating NACs reduction.

5. Conclusion

The present work reported a Fe_3O_4@COOHQ mediated NACs bioreduction process by a novel marine strain, *Shewanella* sp. CNZ-1. Fe_3O_4@COOHQ could be prepared using a green chemical method under mild conditions. Further study showed that Fe_3O_4@COOHQ exhibited good catalytic performance and stability when it was used as a solid-phase mediator for enhancing NACs bioreduction at hypersaline conditions (up to 11% NaCl). The highest NC removal rate of 79.4 mg per h per g cell was achieved at 3% NaCl in the presence of 60 mg L^{-1} Fe_3O_4@COOHQ. Moreover, Fe_3O_4@COOHQ could increase the NC reduction activity of cell membrane proteins (1.71-fold). These findings indicate that the application of strain CNZ-1 and Fe_3O_4@COOHQ is a promising strategy for enhancing the treatment of NACs-containing wastewater containing high concentration of salts.

Acknowledgements

This subject was supported by the National Natural Science foundation of China (No. 51608519), National Natural Science foundation of Shandong Province, China (No. ZR2016EEB10) and the Key Laboratory of Industrial Ecology and Environmental Engineering, China Ministry of Education (KLIEE-16-06).

References

1 K. S. Ju and R. E. Parales, Nitroaromatic compounds, from synthesis to biodegradation, *Microbiol. Mol. Biol. Rev.*, 2010, **74**, 250–274.
2 A. Pandey, P. Singh and L. Iyengar, Bacterial decolorization and degradation of azo dyes, *Int. Biodeterior. Biodegrad.*, 2007, **59**, 73–84.
3 P. Kovacic and S. Ratnasamy, Nitroaromatic compounds: Environmental toxicity, carcinogenicity, mutagenicity, therapy and mechanism, *J. Appl. Toxicol.*, 2014, **34**, 810–824.
4 Ö. S. Kuscu and T. S. Delia, Effects of nitrobenzene concentration and hydraulic retention time on the treatment of nitrobenzene in sequential anaerobic baffled reactor (ABR)/continuously stirred tank reactor (CSTR) system, *Bioresour. Technol.*, 2009, **100**, 2162–2170.
5 A. B. Dos Santos, F. J. Cervantes and J. B. Van Lier, Review paper on current technologies for decolourisation of textile wastewaters: Perspectives for anaerobic biotechnology, *Bioresour. Technol.*, 2007, **98**, 2369–2385.
6 C. M. Carliell, S. J. Barclay, C. Shaw, A. D. Wheatley and C. A. Buckley, The effect of salts used in textile dyeing on microbial decolourisation of a reactive azo dye, *Environ. Technol.*, 1998, **19**, 1133–1137.
7 A. Khalid, F. Kausar, M. Arshad, T. Mahmood and I. Ahmed, Accelerated decolorization of reactive azo dyes under saline conditions by bacteria isolated from Arabian seawater sediment, *Appl. Microbiol. Biotechnol.*, 2012, **96**, 1599–1606.
8 R. Dai, X. Chen, C. Ma, X. Xiang and G. Li, Insoluble/immobilized redox mediators for catalyzing anaerobic bioreduction of contaminants, *Rev. Environ. Sci. Bio/Technol.*, 2016, **15**, 379–409.
9 H. Zhang, H. Lu, S. Zhang, G. Liu, G. Li, J. Zhou and J. Wang, A novel modification of poly(ethylene terephthalate) fiber using anthraquinone-2-sulfonate for accelerating azo dyes and nitroaromatics removal, *Sep. Purif. Technol.*, 2014, **132**, 323–329.
10 J. Wang, H. Lu, Y. Zhou, Y. Song, G. Liu and Y. Feng, Enhanced biotransformation of nitrobenzene by the synergies of *Shewanella* species and mediator-functionalized polyurethane foam, *J. Hazard. Mater.*, 2013, **252**, 227–232.
11 S. Z. Yuan, H. Lu, J. Wang, J. T. Zhou, Y. Wang and G. F. Liu, Enhanced bio-decolorization of azo dyes by quinone-functionalized ceramsites under saline conditions, *Process Biochem.*, 2012, **47**, 312–318.
12 J. B. Guo, J. T. Zhou, D. Wang, C. P. Tian, P. Wang, M. S. Uddin and H. Yu, Biocatalyst effects of immobilized anthraquinone on the anaerobic reduction of azo dyes by the salt-tolerant bacteria, *Water Res.*, 2007, **41**, 426–432.
13 L. Li, J. Wang, J. Zhou, F. Yang, C. Jin, Y. Qu, A. Li and L. Zhang, Enhancement of nitroaromatic compounds anaerobic biotransformation using a novel immobilized redox mediator prepared by electropolymerization, *Bioresour. Technol.*, 2008, **99**, 6908–6916.

14 H. Lu, J. Zhou, J. Wang, W. Si, H. Teng and G. Liu, Enhanced biodecolorization of azo dyes by anthraquinone-2-sulfonate immobilized covalently in polyurethane foam, *Bioresour. Technol.*, 2010, **101**, 7185–7188.

15 L. Alvarez, M. Perez-Cruz, J. Rangel-Mendez and F. Cervantes, Immobilized redox mediator on metal-oxides nanoparticles and its catalytic effect in a reductive decolorization process, *J. Hazard. Mater.*, 2010, **184**, 268–272.

16 L. Alvarez, L. Jimenez-Bermudez, V. Hernandez-Montoya and F. Cervantes, Enhanced dechlorination of carbon tetrachloride by immobilized fulvic acids on alumina particles, *Water, Air, Soil Pollut.*, 2012, **223**, 1911–1920.

17 S. Kango, S. Kalia, A. Celli, J. Njuguna, Y. Habibi and R. Kumar, Surface modification of inorganic nanoparticles for development of organic–inorganic nanocomposites-a review, *Prog. Polym. Sci.*, 2013, **38**, 1232–1261.

18 H. Zhang, H. Lu, J. Wang, T. Zhang, G. Liu and J. Zhou, Transcriptional analysis of *Escherichia coli* during Acid Red 18 decolorization, *Process Biochem.*, 2014, **49**, 1260–1265.

19 I. S. Chang, H. S. Moon, O. Bretschger, J. K. Jang, H. I. Park, K. H. Nealson and B. H. Kim, Electrochemically active bacteria (EAB) and mediator-less microbial fuel cells, *J. Microbiol. Biotechnol.*, 2006, **16**, 163–177.

20 Z. Du, H. Li and T. Gu, A state of the art review on microbial fuel cells: a promising technology for wastewater treatment and bioenergy, *Biotechnol. Adv.*, 2007, **25**, 464–482.

21 B. E. Logan, Exoelectrogenic bacteria that power microbial fuel cells, *Nat. Rev. Microbiol.*, 2009, **7**, 375–381.

22 I. Larsen, B. Little, K. H. Nealson, R. Ray, A. Stone and J. Tian, Manganite reduction by *Shewanella putrefaciens* MR-4, *Am. Mineral.*, 1998, **83**, 1564–1572.

23 O. H. Lowry, N. J. Rosenbrough, A. L. Farr and R. J. Randall, Protein measurement with the Folin phenol reagent, *J. Biol. Chem.*, 1951, **193**, 265–275.

24 M. Solís, A. Solís, H. I. Pérez, N. Manjarrez and M. Flores, Microbial decolouration of azo dyes: a review, *Process Biochem.*, 2012, **47**, 1723–1748.

25 H. Ali, Biodegradation of synthetic dyes-a review, *Water, Air, Soil Pollut.*, 2010, **213**, 251–273.

26 S. N. Singh, *Microbial Degradation of Synthetic Dyes in Wastewaters*, Springer, 2015.

27 F. Xu, Z. Mou, J. Geng, X. Zhang and C. Z. Li, Azo dye decolorization by a halotolerant exoelectrogenic decolorizer isolated from marine sediment, *Chemosphere*, 2016, **158**, 30–36.

28 C. Hessel, C. Allegre, M. Maisseu, F. Charbit and P. Moulin, Guidelines and legislation for dye house effluents, *J. Environ. Manage.*, 2007, **83**, 171–180.

29 J. Rau, H. J. Knackmuss and A. Stolz, Effects of different quinoid redox mediators on the anaerobic reduction of azo dyes by bacteria, *Environ. Sci. Technol.*, 2002, **36**, 1497–1504.

30 H. Lu, H. Zhang, J. Wang, J. Zhou and Y. Zhou, A novel quinone/reduced graphene oxide composite as a solid-phase redox mediator for chemical and biological Acid Yellow 36 reduction, *RSC Adv.*, 2014, **4**, 47297–47303.

31 H. K. Zhang, H. Lu, J. Wang, J. Zhou and S. Meng, Cr(VI) Reduction and Cr(III) immobilization by *Acinetobacter* sp. HK-1 with the assistance of a novel quinone/graphene oxide composite, *Environ. Sci. Technol.*, 2014, **48**, 12876–12885.

32 J. K. Fredrickson, M. F. Romine, A. S. Beliaev, J. M. Auchtung, M. E. Driscoll, T. S. Gardner, K. H. Nealson, A. L. Osterman, G. Pinchuk, J. L. Reed, D. A. Rodionov, J. L. M. Rodrigues, D. A. Saffarini, M. H. Serres, A. M. Spormann, I. B. Zhulin and J. M. Tiedje, Towards environmental systems biology of *Shewanella*, *Nat. Rev. Microbiol.*, 2008, **6**, 592–603.

33 H. Gao, S. Barua, Y. Liang, L. Wu, Y. Dong, S. Reed, J. Chen, D. Culley, D. Kennedy, Y. Yang, Z. He, K. H. Nealson, J. K. Fredrickson, J. M. Tiedje, M. Romine and J. Zhou, Impacts of *Shewanella oneidensis* c-type cytochromes on aerobic and anaerobic respiration, *Microb. Biotechnol.*, 2010, **3**, 455–466.

34 Y. Hong, M. Xu, J. Guo, Z. Xu, X. Chen and G. Sun, Respiration and growth of *Shewanella decolorationis* S12 with an azo compound as sole electron acceptor, *Appl. Environ. Microbiol.*, 2007, **73**, 64–72.